

# DenseNet-SVM: An Intelligent Model for Pancreatic Cancer Detection

Anagani V. Shanthi <sup>1,2,\*</sup>, Alli D. Rani <sup>1,\*</sup>, Panuganti Ravi <sup>3</sup>, and Muppalla Tharangini <sup>4</sup>

<sup>1</sup> Department of Instrument Technology, Andhra University, Visakhapatnam, India

<sup>2</sup> Department of ECE, Vignan's Institute of Engineering for Women (A), Visakhapatnam, India

<sup>3</sup> Department of CSE, Raghu Engineering College (A), Visakhapatnam, India

<sup>4</sup> Department of CSE, GVP College for Degree and PG Courses (A), Visakhapatnam, India

Email: vijayashanthi.anagani@gmail.com (A.V.S.); dr.adaisyrani@andhrauniversity.edu.in (A.D.R.);

panugantiravi@gmail.com (P.R.); ktharangini33@gmail.com (M.T.)

\*Corresponding Author

**Abstract**—Pancreatic Cancer (PC) is a very typical to treat and cure among different type of cancers, which is often found too late and spreads quickly, making survival rates very low. Imaging modalities has mostly been used to diagnose pancreatic cancer, but the most up-to-date imaging gives a bad outlook, which limits the treatments doctors can use. By combining deep learning and machine learning, doctors can make better decisions and find cancer earlier. In this paper, DenseNet 201 a deep learning model and Support Vector Machine (SVM) classifier is utilized for identification of PC. Three stage processing of input data is performed to achieve the results. First stage is data pre-processing; second stage is extraction of features using DenseNet 201 model and reduced using Principal Component Analysis (PCA), final stage is classification using SVM model. The most significant features from the given input image are been extracted using the process of DenseNet 201 model and finalized using PCA before fetching to classifier. The parameters like accuracy, precision, recall, Specificity and F-measure are evaluated. The accuracy obtained using the proposed three stage detection model is 95.52% and is better compared to traditional model. The F1-Score achieved is 94.14 and Area Under the Curve (AUC) is 96.5%.

**Keywords**—pancreatic cancer, Computed Tomography (CT) images, principal component analysis, DenseNet 201, Support Vector Machine (SVM)

## I. INTRODUCTION

Pancreatic cancer is regarded as one of the most-deadly malignancies worldwide. Between the stomach and the spine, in the centre of the abdomen, is a long, flat gland called the pancreas. It is an important part of the digestive system. When cells in the pancreas increase and develop out of control and making a tumour, this is called pancreatic cancer. This is what happens when cells' DNA changes in some way. When a physical examination or imaging tests like a Magnetic Resonance Imaging (MRI) or Computed Tomography (CT) scan are insufficient to

detect malignancy, a biopsy is frequently employed. During this process, a doctor takes a piece of tissue from the patient to look at under a microscope. Tissue samples can be taken in several ways, including through surgery, a needle, or endoscopy.

The five-year mortality rate for people with pancreatic cancer is only 9.3 percent, making it one of the worst cancers that can happen anywhere in the world. The American Cancer Society (2017) says that pancreatic cancer is the main cause of this disease. And the pancreas is one of them. In the gastrointestinal tract, it is the organ that follows the liver. Some fish species have very similar-looking heads, body, and tails. The thickness is only about 5 Centimetres (2 Inches), even when it is fully grown [1, 2]. When the pancreatic exocrine cells proliferate uncontrollably, a disease called pancreatic cancer can happen. This kind of pancreatic cancer happens more often than any other. The tubes and glands that make up exocrine organs are made up of exocrine cells. These organs are in the stomach and keep fluids from leaving the body. The digestive system is home to these exocrine glands, which make enzymes that help break down food [3].

After being released into ducts, which are very thin tubes, enzymes end up in the pancreatic duct, where they stay for good. During digestion, bile made by the liver is pushed out of the body through the ampulla of the Vater. This happens after the bile has gone through the normal bile tube. At some point, the pancreatic duct will reach the normal bile duct and connect to it there. These cells make up a smaller portion of the organ's cells but are essential for making hormones such as glucagon and insulin, which regulate and release sugar levels in blood and then straight into the bloodstream. There are fewer of these cells in the pancreas than there are cells that make up the organ, but they are what make the tumour grow [4].

There are some pancreatic growths that could turn into cancer if they are not addressed, but most of them are normal, which means they do not cause cancer. MRI, CT, ultrasound, Positron Emission Tomography (PET), and PET/CT images that mix PET with CT can help find some types of pancreatic cancer [5]. Fig. 1 shows the

sample CT scan images of normal and PC. Numerous imaging technologies have been created for the medical imaging industry since image processing and computer modelling are the most widely employed techniques in this sector. Researchers who study biological and microbial data still need people to take part in a huge percentage of their studies. Physical processes include the

fact that people tend to have biased views about them, that experts cannot always be trusted, and that procedures take a longer duration and the cost of procedure is high. To do an objective and recursive analysis, you need to use exact numeric measurements, look at very large datasets, and use automatic technologies [6, 7].

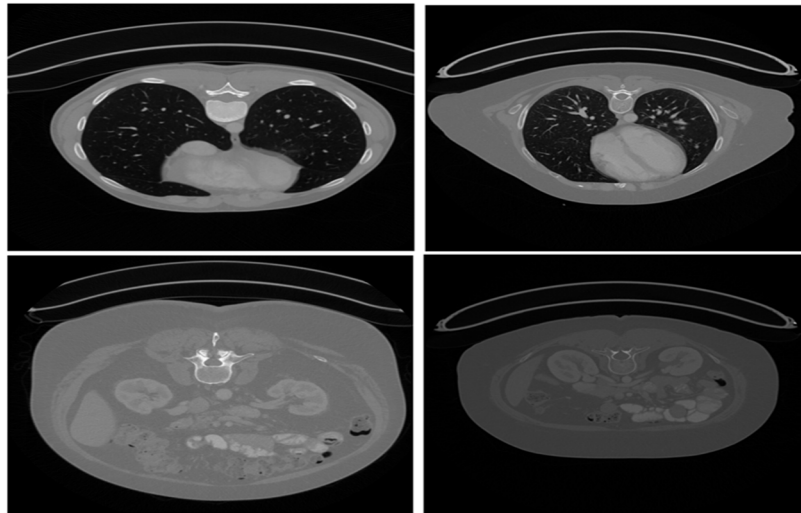


Fig. 1. Example of CT scan image of normal and PC.

Current diagnostic strategies primarily rely on imaging modalities such as CT, MRI, and endoscopic ultrasound, which, despite technological advances, still lack the sensitivity required to detect subtle lesions in the pancreas during the early stages of disease.

In recent years, Artificial Intelligence (AI), particularly Deep Learning (DL) and Machine Learning (ML) methods, has shown significant promise in improving cancer detection and diagnosis. Deep learning models can automatically extract hierarchical features from medical images, thereby enhancing diagnostic performance compared to traditional rule-based algorithms. Among deep learning architectures, DenseNet-201 has been widely used in medical image analysis due to its ability to reuse features across layers and prevent gradient vanishing, leading to better generalization on small and imbalanced datasets like those used in PC detection.

To improve classification accuracy and computational efficiency, feature selection and dimensionality reduction techniques such as Principal Component Analysis (PCA) are often used. PCA helps in retaining the most informative features while eliminating noise and redundancy. Furthermore, Support Vector Machine (SVM), a robust supervised learning algorithm, has been effectively employed for binary classification tasks in medical imaging.

The study's goal is to create a fast, computerised method for grading pancreatic cancer that uses a DL model for pathology pictures. To make a model for correct prediction of pathology pictures, the grading system utilizes a grading level of complex Convolutional Neural Network (CNN) model. The DL model is trained by considering publicly available data source. The model

utilized for training is DenseNet201 along with machine learning method.

The contribution of the study is:

- i. An automated tool is designed using DL and ML techniques to identify the Pancreatic Cancer (PC) in early stage.
- ii. The DL model i.e., DenseNet 201 is designed to identified PC by extracting features of the given pathology input image.
- iii. The ML model i.e., SVM is utilized to differentiate the normal and tumour images and evaluate the metrics.

The rest of the paper discuss about the existing model in identification of PC in Section II, the designed methodology in third section, fourth section discuss the experimental results and finding and finally conclusion is derived in fifth section of the paper.

## II. RELATED WORK

There was new medical research that set the stage and explained why machine learning algorithms and deep learning models are needed for ultrasound images of the pancreas. This was the first part of the literature review. The scope of the work presented in this paper deals with Pancreatic Cancer (PC). The existing models by various authors in identification of PC are reviewed in this section.

Medical imaging has been used a lot to find and diagnose cancerous cells in the digestive system. The current study depends a lot on how knowledgeable and experienced the doctor is. The normal ways of diagnosing are also affected by the quality of the pictures [8]. The field of digital pathology is always changing. The first

generation of image processing tools could only be used to look at a single slide. The second generation of tools, on the other hand, could scan, look at, and store records of whole tissue samples. AI-based algorithms are now the standard way to look at pictures in digital pathology. They can accurately identify the condition and even tell if someone is likely to get the disease before the disease even starts [9]. The scope of AI on medical images helps in identifying the disease and is been utilized to quickly and accurately diagnose the disease [10]. In the case of PC the diagnosis based on AI have been used to predict risk, predict life, tell the difference between cancer masses and other pancreas lesions, and check for reaction after treatment. Machine learning approach for medical image diagnosis discussed by Davatzikos *et al.* [11]. Further machine learning for prediction of risk in PC patients with abnormal morphologic findings is discussed by Chen *et al.* [12].

Extensive investigations have been conducted on machine learning models like Artificial Neural Network (ANN), K-Nearest Neighbour (KNN), and SVM focussing on their capacity to extract distinctive features present in medical image modalities. These signatures hold potential for identifying abnormalities in various types of cancers that are related to digestive system, including PC. The distance between the values of the predefined attributes in the training and sample data is calculated and predicted by the k-NN method, which was first presented by Cover and Hart in 1967. The data sample is categorised according to the computed distance to its closest neighbour class [13]. A separate study utilising k-NN applied a GLCM feature extraction and perform classification in medical imaging for identifying brain tumour and PC [14]. Nonetheless, k-NN faces challenges related to its sensitivity to local structures and the risk of overfitting, which can result in inaccuracies.

Deep learning networks are better at diagnosing than machine learning models because they can take all the traits from medical pictures instead of just a few, which is what machine learning does. Because of this, DL models are better at finding stomach cancers and separating parts of images [15]. CNN is one of the highly utilized models in deep learning concept. These are made up of input layers with groups of nodes that work with hidden layers that all have the same weights and biases and do operations like convolution on the inputs. Each group of nodes works with a different feature. These are then put together and changed to make the result [16].

Liu *et al.* [17] suggests a detailed view of CNN and its layers. CNNs are good at using computers, but they are slow and use a lot of power. It is better to use CNNs for image classification instead of segmentation because they give a probability picture of the whole image [18]. When it comes to the different kinds of CNNs, U-Net algorithms with fewer convolutional layers are often used to diagnose gut cancers, like pancreatic cancer, by sorting and separating certain parts of medical pictures [19]. Between 2012 and 2015, a wide variety of deep learning models were produced, including AlexNet, VGGNet,

Inception Net, and ResNet. The number of convolutional and pooling layers they employ varies [20].

In the case of cancers that are related to digestive system, Sharma *et al.* [21] used the AlexNet design to accurately classify and find necrosis in medical pictures of gastric carcinoma with a success rate of 69.9% for classification and 81% for detection. Shin *et al.* [22] used the Inception-Resnet network to automatically find colonic polyps in test pictures.

The progress made in the DL model makes it possible to quickly and automatically find many basic traits that can only be found by medical experts doing a lot of work by hand. Transfer learning makes DL very flexible so it can be used in a lot of different situations. For instance, during the recent pandemic Covid-19, DL utilization made easy and quick to find the positives cases and which helped in stopping wide spread of disease by detecting accurately [23]. To get valuable information, such as morphological characteristics on WSI, to identify cancer conditions and classify them into two or more categories, the detection and classification of malignant cells in pathological images using DL has been employed extensively [24]. A lot of tasks can be automated with DL, but different models will work with different biomarkers and stain types in different ways. DL is the best at accurately identifying tumours, using computers quickly, and applying its findings to a wide range of pathological pictures. It is especially good at segmentation (finding tumour regions), detection (finding metastases), and classification (grading cancer and predicting patient outcome).

Computerised Tomography (CT) is the main way that pancreatic cancer is found and evaluated, but it depends a lot on how experienced the doctors are. Liu *et al.* [25] using a CNN, DL can help correctly tell the difference between PC and non-PC using the CT images. Locating tiny cancers (less than 2 cm) was the challenge. The authors developed a detection technique based on patches. They discovered that the ideal patch size for detecting pancreatic tumours on CT was 50 by 50 pixels, or 3.5 by 3.5 cm. There are many more studies on the topic of using CT to grade pancreatic cancer that can be found in the journals. Chu *et al.* [26] did a study on how to use advanced visualisation methods to find pancreatic cancer more quickly using DL. A way to use Principal Component Analysis (PCA) [27] and K-means grouping [28] to separate and retrieve features from medical pictures. The portions of the image that are most crucial to the research are divided using this technique. K-means is a way to group things together, and it can be used to find important parts of a picture. One way to improve accuracy is to use PCA more in the process of extracting the features and identifying the best possibilities of groups. To effectively improve the rate of detection, combination of PCA, deep learning (DenseNet 201) and machine learning (SVM) is proposed in this work and the model is discussed in next section.

### III. METHOD

Pancreatic Cancer (PC) is a type of disease that develop in the pancreas, a vital organ located in the abdomen behind the stomach. The pancreas plays a

critical role in digestion by producing enzymes and regulating blood sugar levels through hormone production. Early detection and diagnosis are very much essential for the survival of patients. The model utilized for detection of PC is shown in Fig. 2 and is discussed.

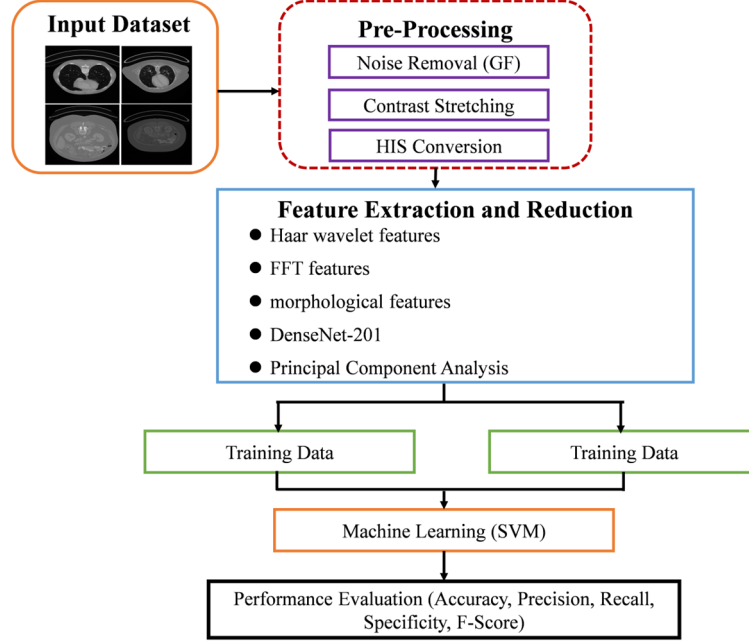


Fig. 2. Design flow of proposed model.

#### A. Dataset

Doctors' records are very private, and the best sample should be used to test the method for finding problems. This study used a collection with pictures of the pancreas for two types: healthy and pancreatic cancer. The data set came from Kaggle data, an open-source library. The National Institutes of Health Clinical Centre (NIHCC) did 82 belly contrast-enhanced 3D CT pictures on 53 men and 27 women, about 70 Seconds after injecting contrast into their veins (Table I). In this study, 17 healthy kidney donors were scanned before they had a nephrectomy. A radiologist chose the other 65 patients from people who did not have big stomach problems or pancreatic cancer lesions. People in the study are between the ages of 18 and 76, with  $46.8 \pm 16.7$  being the mean age. The CT scans were taken on Philips and Siemens MDCT machines (120 kVp tube voltage) and have resolutions of  $512 \times 512$  pixels with different sizes of pixel and thicknesses of slice in mm i.e., 1.5 to 2.5 [29].

TABLE I. ANALYSIS OF DATASET

Attribute	Description
Samples	82 contrast-enhanced 3D abdominal CT scans
No of patients	82 patients (53 males, 27 females)
Age	18–76 years (Mean: $46.8 \pm 16.7$ years)
Resolution	$512 \times 512$ pixels
Slice thickness	1.5–2.5 mm
Healthy case	17 healthy kidney donors
Abnormal cases	65 patients without major abdominal issues or pancreatic lesions
Data sources	Open-source Kaggle dataset (NIH Clinical Center origin)

#### B. Preprocessing

This stage is very crucial to improvise the early-stage identification of PC. In this step, the input dataset images are converted into hyperspectral images. In this step, Gaussian Filtering (GF) is used to get rid of the unwanted noise in the pictures, which makes it easier to focus on the problem that was set. The data is ready for the next step by keeping all its specific information. The gaussian filter is made up of kernels that come from the gaussian function in Eq. (1).

$$G(x, y) = \frac{1}{2\pi\sigma^2} e^{-\frac{x^2+y^2}{2\sigma^2}} \quad (1)$$

where,  $x, y$  are the coordinates in the kernel.  $\sigma$  is termed as Standard Deviation (SD) and improved level of smoothing if SD is greater.

In this stage, Contrast Stretching is used to improve an image's contrast by making the range of strength values bigger to fit a certain range. It is often used to make details in an image stand out more or get data ready for more research. When you stretch the contrast, the pixel intensities in an image are changed from their original range to a larger or more specific range. This range is usually the whole possible value range, like 0–255 for an 8-bit image. The change can be either linear or not linear. There is a linear contrast stretching, and Eq. (2) shows how the strength changes.

$$I_o = \frac{(I_i - I_{min})}{(I_{max} - I_{min})} \cdot (O_{max} - O_{min}) + O_{min} \quad (2)$$

where,  $I_o$  is the improved intensity level output,  $I_i$  is the pixels intensity of the given input,  $I_{min}$  is the inputs minimum intensity level,  $I_{max}$  is the inputs maximum intensity level,  $O_{min}$  is the minimum desired intensity level of the output,  $O_{max}$  is the output desired level of intensity which is maximum.

To improve the discriminative power of standard CT images, we introduce a hyperspectral transformation step, in which each CT image is processed into a hyperspectral-like format. This technique expands the spatial grayscale image into multiple synthetic spectral bands using filter-based or transformation-based methods. Recent studies have shown that such conversions improve tumor detectability by allowing models to learn spectral and textural variations more effectively for performing surgeries [30].

This pseudo-HSI representation is particularly beneficial in enhancing deep learning models' ability to distinguish fine-grained anatomical structures and tumor boundaries in low-contrast CT images. This process helps in improving the performance of classifier.

### C. Feature Extraction

In image process the extraction of features is the process of finding and extracting unique and important information from a picture so that its content can be shown clearly. This process takes away some of the data's complexity while keeping the important details needed for analysis or other tasks, like sorting and finding the result that is wanted. In this paper, the features are

extracted using two model one is Principal Component Analysis (PCA) and other is DenseNet 201. Some of the features like Haar wavelet features, FFT features and morphological features are also extracted.

The Haar wavelet is the simplest wavelet. It represents data with step functions. It divides an image into estimate coefficients, which show the big picture or low-frequency parts, and detail coefficients, which show the small details or high-frequency parts in all three directions (horizontally, vertically, and diagonally).

Using the Fourier Transform, a math tool that changes data in domain of time or space to the domain of frequency. Fast Fourier Transform (FFT) features are taken from images that are fed into it. A lot of people use these tools to process pictures, and they will help find PCs. These traits also help the machine learning model look for trends, frequencies, or recurring events in the data. In image analysis, morphological features are features that are extracted using morphological operations, which look at and change the shape of a certain area in a picture. Shape, size, orientation, and connectivity of pixels are taken out, which makes them very useful for the suggested medical imaging model for PC recognition.

#### 1) DenseNet-201

The DenseNet design is a DNN that links each layer-by-layer in a way called "feed-forward". Traditional designs, like ResNet, only connect each layer to the next one. DenseNet layers, on the other hand, connect to many other layers [31]. In this study, DenseNet-201 is mainly used to access all the features of the input CT picture. The network has access to all past feature maps, which makes it easier to reuse features and cuts down on the need for doing the same work twice. The representation of proposed DenseNet-201 is shown in Fig. 3.

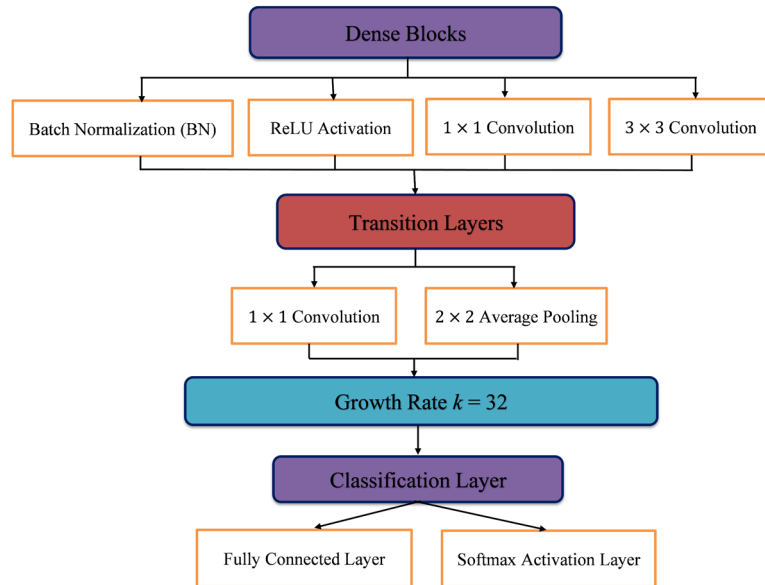


Fig. 3. Structure of DensNet-201 model.

The layers and the configuration details of the proposed model is been discussed. The convolutional layer with  $7 \times 7$ , 64 and 2 strides, the output size is  $112 \times 112$ . Next layer is max pooling with  $3 \times 3$ , 2 strides

having output size of  $56 \times 56$ . Now densenet layers are as Dense Block1 (DB1) with configuration of  $6 \times [BN, ReLU, 1 \times 1, 3 \times 3]$ , the output size is  $56 \times 56$ . Transition Layer1 (TL1) with a config of  $1 \times 1$  convolution and  $2 \times 2$  pooling,



the output size is  $28 \times 28$ . Now repeat DB and TL. The configuration of DB2 is  $12 \times [BN, ReLU, 1 \times 1, 3 \times 3]$  with output of  $28 \times 28$ . TL2 with a config of  $1 \times 1$  convolution and  $2 \times 2$  pooling, the output size is  $14 \times 14$ . DB3 with config of  $48 \times [BN, ReLU, 1 \times 1, 3 \times 3]$ , the output size is  $14 \times 14$ . TL3 with a config of  $1 \times 1$  convolution and  $2 \times 2$  pooling, the output size is  $7 \times 7$ . DB4 with config of  $32 \times [BN, ReLU, 1 \times 1, 3 \times 3]$ , the output size is  $7 \times 7$ . The global avg pooling with a size of  $7 \times 7$  pooling, output size is  $1 \times 1$ . Finally full connected layer with softmax output

and the size is  $1 \times 1$ . The densenet model mainly concentrates on the shape feature which helps in identifying the PC more accurately. The features extracted using PCA and DenseNet 201 and other features are combined and are fetched to classification model. Higher accurate features help in achieving higher rate in detection of PC.

The summary of DenseNet 201 model is simplified and tabulated in Table II.

TABLE II. SUMMARY OF DENSENET 201 MODEL

Stage	Type of layer	Output	Process
Input	Input Image	$224 \times 224 \times 3$	Input CT image
Convolution	$7 \times 7$ conv, filter-64, stride 2	$112 \times 112 \times 64$	Initial Feature extraction
Pooling	$3 \times 3$ max pooling, stride 2	$56 \times 56 \times 64$	Downsampling
DB1	$6 \times [BN, ReLU, 1 \times 1 \text{ conv}, 3 \times 3 \text{ conv}]$	$56 \times 56 \times 256$	First Dense Block
TL1	$1 \times 1$ Conv + $2 \times 2$ Avg Pooling	$28 \times 28 \times 128$	Reduces size and compresses features
DB2	$12 \times [BN, ReLU, 1 \times 1 \text{ Conv}, 3 \times 3 \text{ Conv}]$	$28 \times 28 \times 512$	Second dense block
TL2	$1 \times 1$ Conv + $2 \times 2$ Avg Pooling	$14 \times 14 \times 256$	-
DB3	$48 \times [BN, ReLU, 1 \times 1 \text{ Conv}, 3 \times 3 \text{ Conv}]$	$14 \times 14 \times 1024$	Third dense block
TL3	$1 \times 1$ Conv + $2 \times 2$ Avg Pooling	$7 \times 7 \times 512$	-
DB4	$32 \times [BN, ReLU, 1 \times 1 \text{ Conv}, 3 \times 3 \text{ Conv}]$	$7 \times 7 \times 1920$	Final Dense Block
Global pooling	$7 \times 7$ Global Average Pooling	$1 \times 1 \times 1920$	Convert feature map to vector
Fully connected	Dense Layer+Softmax	$1 \times 1 \times \text{classes}$	Output classification probability

## 2) Principal component analysis

The extraction process of feature for HIS images is performed using PCA. PCA is a way to reduce the number of dimensions that are used in picture processing and data analysis. Finding the paths of the data's highest variance changes it into a new set of traits that are not related to each other. These are called principal components. PCA pulls out features by projecting data onto an area with fewer dimensions while keeping as much data as possible. Process of PCA feature extraction is shown in Fig. 4. It doesn't matter what size you use for the PCA, and the picture features have a mean of 0 and a standard deviation of 1. Covariance is used to figure out how the picture properties are related to each other. You can change the data into a new feature space defined by the chosen main components by using eigenvectors to show the lines of variance and eigenvalues to show the values how much variation there is along each eigenvector.

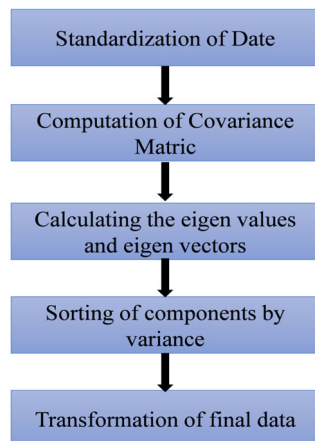


Fig. 4. Process of PCA.

The eigenvalues of each component are used to rank them. The ' $k$ ' best components with the highest eigenvalues are chosen. Features like sides, edges, and noisy patterns are not considered. Features that come highly suggested are sent for training and testing.

## D. Classification Model

The classification model designed to identify the PC is Support Vector Machine (SVM). SVM is well known classifier which performance shows better results in many scenarios. The SVM hyperplane model that was used to get the results. The best hyperplane for separating classes with the most space between them. The important data points that are close to the choice line are the support vectors. The success measures depend on the hyperplane as the data points close to the plane are considered. The data available is utilized by classifier for training and testing in the ratio of 70:30. The process of classification is detailed in Fig. 5.

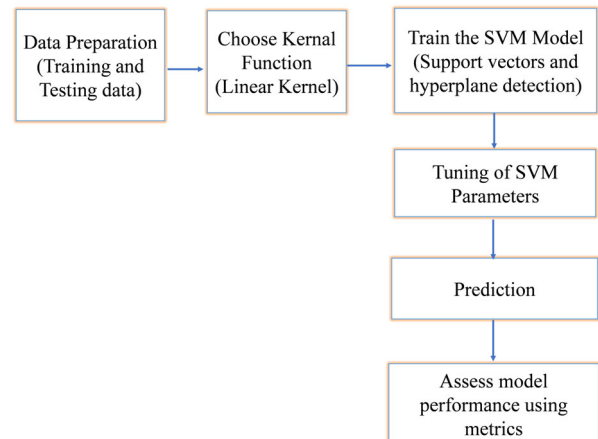


Fig. 5. Process flow of SVM model.

A 5-fold cross-validation is performed in our evaluation process. The dataset was partitioned into five equal subsets, and the training and evaluation were repeated five times, each time using a different subset for testing and the remaining for training. The reported metrics—accuracy, precision, recall, specificity, and F1-Score—are now averaged over the five folds.

#### IV. RESULTS AND DISCUSSION

##### A. System Environment

A 16GB RAM system with an Intel Core 2.60 GHz CPU was used to write and execute the automated detection method in MATLAB. Using adaptive deep learning on hyperspectral images, we presented an automated pancreatic cancer detection approach in this research.

To differentiate between malignant and normal tissue, a DCNN network framework is used to extract deep features from  $390 \times 435 \times 251$  hyperspectral images.

The proposed model specifically utilized the Adam optimizer with a learning rate of 0.0001, batch size of 32,

and trained the model for 50 epochs. To avoid overfitting, dropout regularization with a rate of 0.5 was applied, along with early stopping based on validation loss.

##### B. Experimental Results

The results obtained in the process of detection of PC is discussed below. The Densenet-201 model uses four dense blocks and three transition layers to achieve the results expected. The input image and its HSI with no cancer is shown in Fig. 6, with cancer input image and HIS image is shown in Fig. 7.

Fig. 6 presents the original input CT image and its corresponding Hyper-Spectral Image (HSI) representation for a non-pathological (non-cancerous) case. The HSI conversion simulates enhanced spectral resolution by generating pseudo-spectral bands, enabling the model to capture subtle tissue heterogeneities and spectral signatures not visible in standard grayscale imaging. This transformation provides a richer input for downstream feature extraction, even in the absence of malignant anomalies.

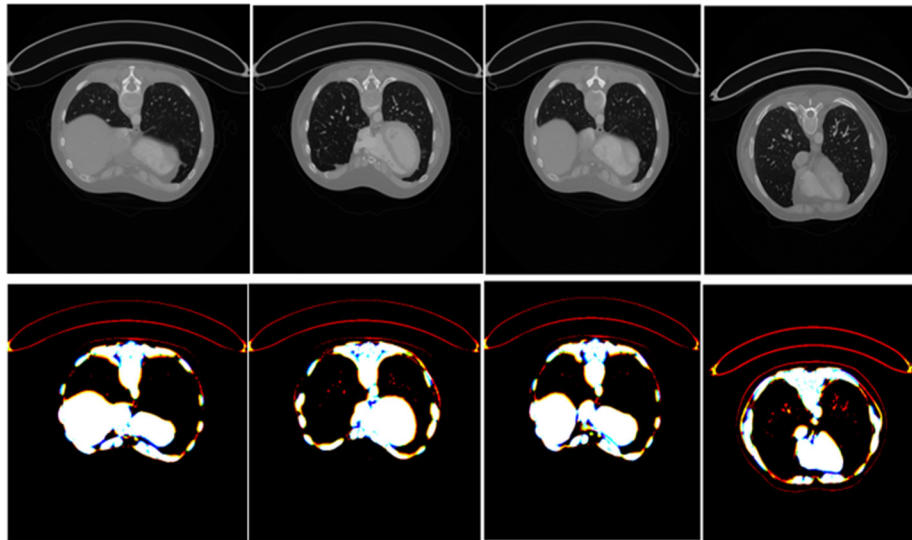


Fig. 6. Input and hyperspectral images with no cancer.

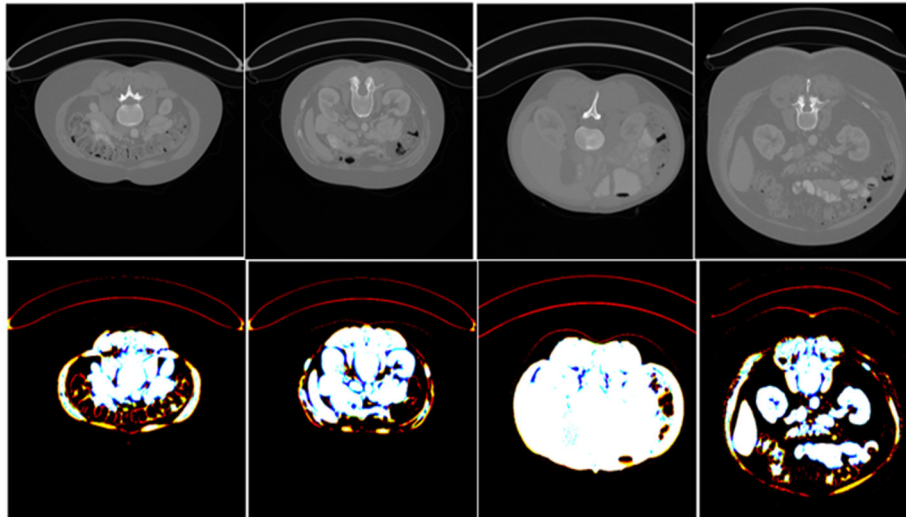


Fig. 7. Input and hyperspectral images with pancreatic cancer.





Fig. 7 displays the input CT image alongside its corresponding HSI representation for a cancerous case. The HSI transformation augments the spectral resolution of the image, allowing for enhanced visualization of pathological tissue characteristics. This spectral enrichment facilitates the deep learning model in detecting subtle spectral and spatial anomalies associated with malignant regions, thereby improving the sensitivity

of the diagnostic process. The parts of HIS pictures that are improved help the model get a higher rate of accuracy and make early process diagnoses. Pathologists can use the computer-aided prediction model to help them automate the time-consuming process of manually identifying cancer from pathology photos. The validation loss for existing model and proposed model is compared and is shown in Fig. 8.

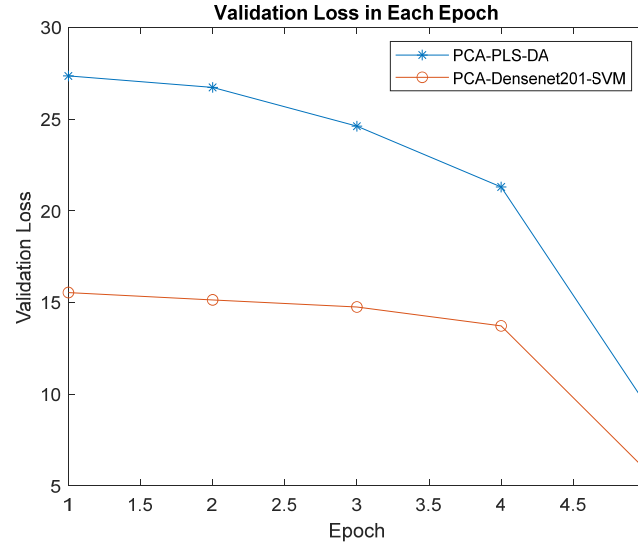


Fig. 8. Analysis of validation loss.

From Fig. 8 validation loss is inversely proportional to the number of epochs. For example, at epoch 5 the validation loss of proposed model is 6% whereas at epoch 1 the validation loss is 15.5%. The lowest validation loss is seen using PCA-DenseNet 201 compared to PCA-PLS-DA existing model.

### C. Parametric Evaluation

The parameters evaluated are Accuracy, specificity, precision, recall and F-Score. The evaluation of these parameters performed using the following Eqs. (3)–(7) respectively.

$$Acc = \frac{Tp + Tn}{Tp + Tn + Fp + Fn} \quad (3)$$

$$Sp = \frac{Tn}{Tn + Fp} \quad (4)$$

$$Pr = \frac{Tp}{Tp + Fp} \quad (5)$$

$$Re = \frac{Tp}{Tp + Fn} \quad (6)$$

$$F - Score = 2 \times \frac{Pr \times Re}{Pr + Re} \quad (7)$$

where  $Tp$  is Truly positive,  $Tn$  is Truly negative,  $Fp$  is

Falsely positive,  $Fn$  is Falsely negativity. The evaluation shows the validity and effectiveness of the proposed methodology. Higher the values achieved more the effectiveness of the model in detection of PC. The results obtained after performing PCA-DCNN-SVM operation is shown in Table III.

TABLE III. EVALUATION METRICS OF THE DESIGNED MODEL

Parameter/ Technique	PCA-PLS- DA	U-Net	ResNet- SVM	Proposed PCA- DCNN-SVM
Accuracy (%)	90.50	91.86	93.67	<b>95.52</b>
Specificity (%)	92.44	92.45	94.56	<b>96.09</b>
Precision (%)	89.83	91.9	93.82	<b>94.79</b>
Recall (%)	91.0	91.74	92.36	<b>93.59</b>
F-Score (%)	88.8	92.35	92.85	<b>94.14</b>

Area Under the Curve (AUC) evaluates how well a model can distinguish between classes. It measures the area under the Receiver Operating Characteristic (ROC) curve, which plots the True Positive Rate (Recall) against the False Positive Rate. The AUC value achieved is 96.5% for PC class and 95.1% for normal class.

One way to measure how well a classifier does at a task is to look at the confusion matrix, which compares actual (true) labels to predicted labels. This is especially helpful for seeing how well a model does at multi-class classification tasks. The confusion matrix achieved for existing model and proposed DCNN-SVM model and is shown in Fig. 9.

The confusion matrix shown in Fig. 9 specifically, the class-wise performance in terms of true positives, false positives, true negatives, and false negatives. For

example, the model demonstrates strong sensitivity (true positive rate) in correctly identifying pancreatic cancer cases, with relatively few false negatives, indicating reliable cancer detection. However, a small number of

false positives (i.e., healthy cases misclassified as cancer) were observed, which could be further reduced by fine-tuning classification thresholds or incorporating more diverse training data.

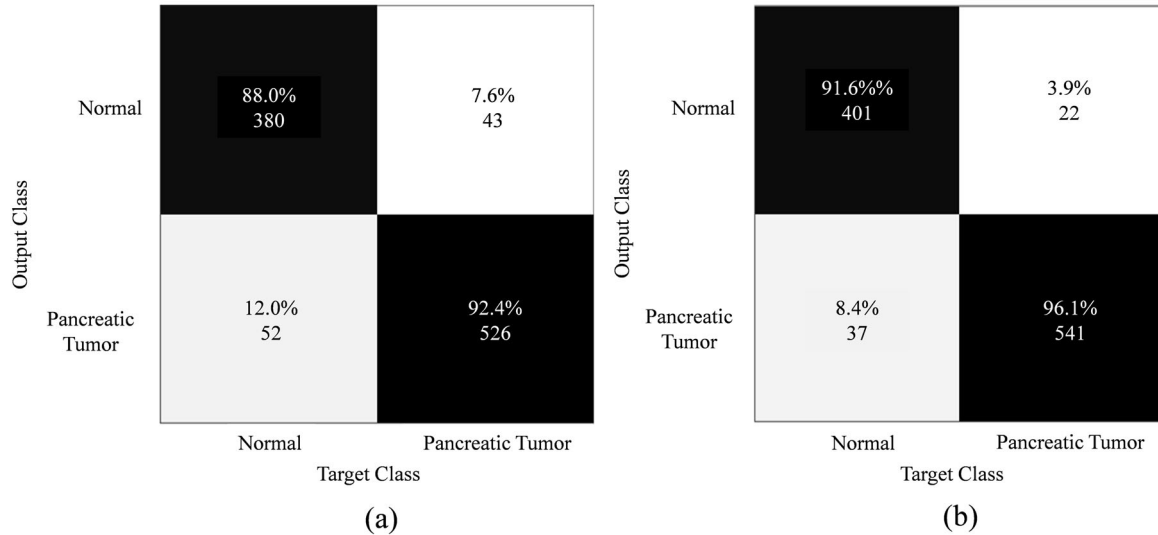


Fig. 9. Confusion matrix for (a) PCA-PLS-DA model, (b) DCNN-PCA-SVM model.

To test the efficiency of linear kernel, the model is evaluated using different SVM kernels and the accuracy achieved using different kernels is shown in Table IV.

TABLE IV. ACCURACY USING DIFFERENT SVM KERNELS

SVM kernel /Metric	Accuracy (%)
Linear Kernel	95.52
RBF	92.37
Polynomial	90.82
Sigmoid	89.59

The comparison of performance metrics for existing tradition model with the proposed integration of DL and ML is shown in Fig. 10.

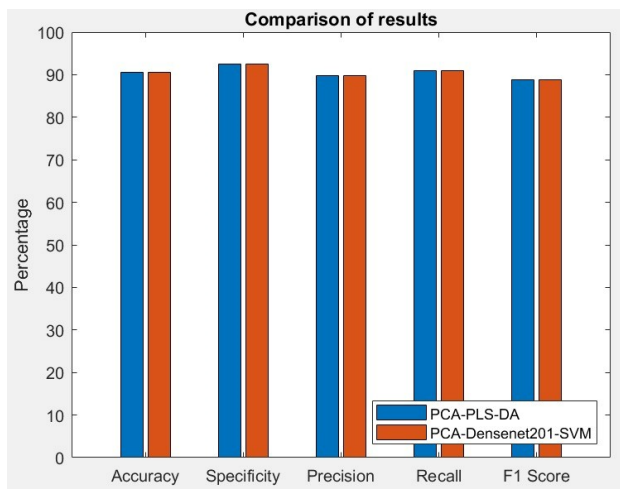


Fig. 10. Comparison of parametric of two models.

The comparison of accuracy in identification of PC in existing model and the value achieved using proposed model is shown in Fig. 11. When compared with existing models proposed model having an accuracy of 94.52%

which is 13.4% higher compared to Gao and Wang [32] and 17.7% higher when compared to Gao and Wang [33]. The nearest accuracy achieved is 90.2% [34] which is 4.3% less compared to our proposed model.

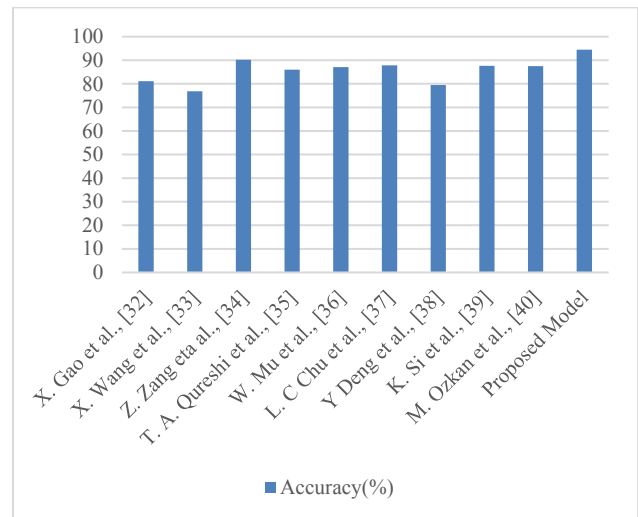


Fig. 11. Accuracy comparison.

Some of the existing deep learning models and classification models in identification of PD is also compared and is shown in Table V. The techniques used in this paper having good accuracy which can be further implemented for identification of PD.

To validate the comparative performance of our proposed model against other baseline deep learning architectures, we conducted a statistical significance analysis using a paired t-test. The test yielded a t-value of 0 and a p-value of 1, indicating that there is no statistically significant difference between the models' performances on the evaluated dataset. This suggests that,

while our model achieves high accuracy, its performance is comparable to existing architectures under the current experimental settings.

TABLE V. ACCURACY USING DIFFERENT TECHNIQUES

Author and Ref	Technique	Acc (%)
Maskeliunas <i>et al.</i> [41]	U-LossianNet	94.3
Quan <i>et al.</i> [42]	2D CNN + 1D CNN	92
Yasar <i>et al.</i> [43]	ANN	94.9
Nissar <i>et al.</i> [44]	XG Boost	95.3
Yuan <i>et al.</i> [45]	DNN Ensemble	95
Mathur <i>et al.</i> [46]	KNN+AdaBoost M1	91.28

## V. ABLATION STUDY

The study aims to identify how every technique is useful in improving the detection accuracy. In this study the experiment conducted on different cases and evaluated the accuracy result.

Case1. Accuracy in detection of PC without using DenseNet 121 and tested the contribution. The accuracy obtained is 92.46%.

Case2. No DenseNet 121. Directly utilized raw features and classified using SVM. The rate of accuracy achieved is 90.52%.

Case3. The model designed with extracting features, utilized only DenseNet 121 and performed classification using SVM for detection of PC. The rate of accuracy obtained is 94.26%.

Case4. In addition, PCA is included for reduction of extracted features along with DenseNet-SVM model and achieved an accuracy of 95.52%.

From this study the combination of DenseNet 121-PCA-SVM provides better detection accuracy.

While the proposed framework demonstrates high accuracy and strong performance in pancreatic cancer classification, several limitations and real-world challenges must be acknowledged:

**Computational Complexity:** The integration of DenseNet-201 with hyperspectral imaging and PCA significantly increases computational demands. DenseNet-201, being a deep architecture with densely connected layers, requires considerable memory and GPU resources for both training and inference, making it less feasible for real-time or resource-constrained environments.

**Dataset Size and Variability:** The dataset used in this study is relatively limited in size and sourced from a controlled, homogeneous population. This restricts the generalizability of the model to wider clinical scenarios where imaging protocols, scanner types, and patient demographics vary. Further evaluation on multi-institutional and heterogeneous datasets is necessary to ensure robust performance across clinical environments.

The modular design of the proposed framework combining hyperspectral representation, DenseNet-201 for deep feature extraction, PCA for dimensionality reduction, and SVM for classification offers flexibility for adaptation to other types of cancer and broader medical imaging tasks.

The model can be trained on CT, MRI, or PET datasets associated with lung, liver, or brain cancers, provided

appropriate ground truth labels and pre-processing pipelines. Hyperspectral transformation techniques can similarly be applied to enhance tumor visibility in these modalities.

## VI. CONCLUSION

It is a very dangerous disease that can be found anywhere in the world, and only a small percentage of people who get it survive for five years. It is possible to identify illnesses like pancreatic cancer if they are found early on. Having more medical imaging tests available has made it possible for a good number of cancer patients to find problems earlier. For a lot of people, the technology is out of reach because the equipment and facilities needed are very expensive. This makes it hard to spread. This paper discusses the utilization of a DL model and machine learning model in image processing for identifying the PC by considering the CT images. The preprocessing stage all the input images are converted to HSI and processed. The features are extracted using PCA and Densenet-201 model and finally classified using support vector machine classified. The F1-Score obtained using the proposed model is 94.14% and the rate of accuracy is 95.52%. By using the designed model, the outcome of patients with PC will be improved. To improve PC diagnosis and patient results, we also need to come up with more accurate and non-invasive screening methods. Standardised scoring systems are also very important. Future work will focus on scaling the dataset, improving computational efficiency, enhancing interpretability with visualization tools, and validating the framework on real-world clinical data to bridge the gap between research and clinical practice. Also explore the possibility of integrating other deep learning architectures or hybrid models to further improve accuracy and reduce validation loss.

## CONFLICTS OF INTEREST

The authors declare no conflict of interest.

## AUTHOR CONTRIBUTIONS

Anagani Vijaya Shanthi conducted the research work, collected the data, and wrote the paper. Alli Daisy Rani supervised the work. Panuganti Ravi and Muppala Tharangini reviewed and corrected the details of the paper. All authors had approved the final version.

## REFERENCES

- [1] G. Suman, A. Patra, P. Korfiatis *et al.*, "Quality gaps in public pancreas imaging datasets: Implications & challenges for AI applications," *Pancreatol.*, vol. 21, no. 5, pp. 1001–1008, 2021.
- [2] P. T. Chen, D. Chang, H. Yen *et al.*, "Radiomic features at CT can distinguish pancreatic cancer from noncancerous pancreas," *Radiol. Imaging Cancer*, vol. 3, no. 4, e210010, 2021.
- [3] G. Suman, A. Panda, P. Korfiatis, and A. H. Goenka, "Convolutional neural network for the detection of pancreatic cancer on CT scans," *Lancet Digit. Health*, vol. 2, no. 9, e453, 2020.
- [4] V. Jasti, A. Zamani, K. Arumugam *et al.*, "Computational technique based on machine learning and image processing for

- medical image analysis of breast cancer diagnosis,” *Secur. Commun. Netw.*, vol. 2022, no. 7, 1918379, 2022.
- [5] P. Ryan, T. S. Hong, and N. Bardeesy, “Pancreatic adenocarcinoma,” *N. Engl. J. Med.*, vol. 371, no. 11, pp. 1039–1049, 2014.
- [6] B. Kenner, S. T. Chari, D. Kelsen *et al.*, “Artificial intelligence and early detection of pancreatic cancer,” *Pancreas*, vol. 50, no. 3, pp. 251–279, 2021.
- [7] S. Chaudhury, A. N. Krishna, S. Gupta *et al.*, “Effective image processing and segmentation-based machine learning techniques for diagnosis of breast cancer,” *Comput. Math. Methods Med.*, vol. 2022, no. 1, 6841334, 2022.
- [8] S. Gassenmaier, S. Afat, D. Nickel *et al.*, “Deep learning–accelerated T2-weighted imaging of the prostate: Reduction of acquisition time and improvement of image quality,” *Eur. J. Radiol.*, vol. 137, 109600, 2021.
- [9] M. J. Iqbal, Z. Javed, H. Sadia *et al.*, “Clinical applications of artificial intelligence and machine learning in cancer diagnosis: Looking into the future,” *Cancer Cell Int.*, vol. 21, p. 270, 2021.
- [10] J. Xu, M. Jing, S. Wang, C. Yang, and X. Chen, “A review of medical image detection for cancers in digestive system based on artificial intelligence,” *Expert Rev. Med. Devices*, vol. 16, no. 10, pp. 877–889, 2019.
- [11] C. Davatzikos, A. Sotiras, Y. Fan *et al.*, “Precision diagnostics based on machine learning-derived imaging signatures,” *Magn. Reson. Imaging*, vol. 64, pp. 49–61, 2019.
- [12] W. Chen, Q. Chen, R. A. Parker *et al.*, “Risk prediction of pancreatic cancer in patients with abnormal morphologic findings related to chronic pancreatitis: A machine learning approach,” *Gastro. Hep. Adv.*, vol. 1, no. 6, pp. 1014–1026, 2022.
- [13] E. Avuçlu and A. Elen, “Evaluation of train and test performance of machine learning algorithms and Parkinson diagnosis with statistical measurements,” *Med. Biol. Eng. Comput.*, vol. 58, pp. 2775–2788, 2020.
- [14] J. Reddy, T. A. Prasath, M. P. Rajasekaran, and G. Vishnuvarthanan, “Brain and pancreatic tumor classification based on GLCM—K-NN approaches,” in *Proc. Int. Conf. Intell. Comput. Appl.*, 2019, vol. 846, pp. 293–302.
- [15] W. Du, N. Rao, D. Liu *et al.*, “Review on the applications of deep learning in the analysis of gastrointestinal endoscopy images,” *IEEE Access*, vol. 7, pp. 142053–142069, 2019.
- [16] P. Kim, “Convolutional neural network,” in *Proc. MATLAB Deep Learning*, 2017, pp. 121–147.
- [17] Y. H. Liu, “Feature extraction and image recognition with convolutional neural networks,” *J. Phys. Conf. Ser.*, vol. 1087, 062032, 2018.
- [18] A. Kumar, J. Kim, D. Lyndon, M. Fulham, and D. Feng, “An ensemble of fine-tuned convolutional neural networks for medical image classification,” *IEEE J. Biomed. Health Inform.*, vol. 21, no. 1, pp. 31–40, 2017.
- [19] N. Siddique, S. Paheding, C. P. Elkin, and V. Devabhaktuni, “U-Net and its variants for medical image segmentation: A review of theory and applications,” *IEEE Access*, vol. 9, pp. 82031–82057, 2021.
- [20] F. Özyurt, “A fused CNN model for WBC detection with MRMR feature selection and extreme learning machine,” *Soft Comput.*, vol. 24, pp. 8163–8172, 2020.
- [21] H. Sharma, N. Zerbe, I. Klempert, O. Hellwich, and P. Hufnagel, “Deep convolutional neural networks for automatic classification of gastric carcinoma using whole slide images in digital histopathology,” *Comput. Med. Imaging Graph.*, vol. 61, pp. 2–13, 2017.
- [22] Y. Shin, H. A. Qadir, L. Aabakken, J. Bergsland, and I. Balasingham, “Automatic colon polyp detection using region based deep CNN and post learning approaches,” *IEEE Access*, vol. 6, pp. 40950–40962, 2018.
- [23] W. M. Bahgat, H. M. Balaha, Y. AbdulAzeem, and M. M. Badawy, “An optimized transfer learning-based approach for automatic diagnosis of Covid-19 from chest X-ray images,” *PeerJ Comput. Sci.*, vol. 7, p. e555, 2021.
- [24] A. R. Bhatt, A. Ganatra, and K. Kotecha, “Cervical cancer detection in Pap smear whole slide images using ConvNet with transfer learning and progressive resizing,” *PeerJ Comput. Sci.*, vol. 7, e348, 2021.
- [25] K. L. Liu, T. Wu, P. T. Chen *et al.*, “Deep learning to distinguish pancreatic cancer tissue from non-cancerous pancreatic tissue: A retrospective study with cross-racial external validation,” *Lancet Digit. Health*, vol. 2, no. 6, pp. e303–e313, 2020.
- [26] L. C. Chu, S. Park, S. Kawamoto, A. L. Yuille, R. H. Hruban, and E. K. Fishman, “Pancreatic cancer imaging: A new look at an old problem,” *Curr. Probl. Diagn. Radiol.*, vol. 50, no. 4, pp. 540–550, 2021.
- [27] K. Szymoński, K. Skirlińska-Nosek, E. Lipiec *et al.*, “Combined analytical approach empowers precise spectroscopic interpretation of subcellular components of pancreatic cancer cells,” *Anal. Bioanal. Chem.*, vol. 415, pp. 7281–7295, 2023.
- [28] R. R. Reena and G. S. A. Mala, “An improved K-means clustering for segmentation of pancreatic tumor from CT images,” *IETE J. Res.*, vol. 69, no. 7, pp. 3966–3973, 2021.
- [29] H. Roth, A. Farag, E. B. Turkbey, L. Lu, J. Liu, and R. M. Summers, “Data from pancreas-CT (Version 2),” *The Cancer Imaging Archive*, 2016. <https://doi.org/10.7937/K9/TCIA.2016.tNB1kqBU>
- [30] S. Puustinen, H. Vrzáková, J. Hyttinen *et al.*, “Hyperspectral imaging in brain tumor surgery—Evidence of machine learning-based performance,” *World Neurosurgery*, vol. 175, pp. e614–e63, 2023. <https://doi.org/10.1016/j.wneu.2023.03.149>
- [31] G. Huang, Z. Liu, L. V. D. Maaten, and K. Q. Weinberger, “Densely connected convolutional networks,” in *Proc. IEEE Conf. Comput. Vis. Pattern Recognit. (CVPR)*, 2017, pp. 2261–2269.
- [32] X. Gao and X. Wang, “Deep learning for World Health Organization grades of pancreatic neuroendocrine tumors on contrast-enhanced magnetic resonance images: A preliminary study,” *Int. J. Comput. Assist. Radiol. Surg.*, vol. 14, pp. 1981–1991, 2019.
- [33] X. Gao and X. Wang, “Performance of deep learning for differentiating pancreatic diseases on contrast-enhanced magnetic resonance imaging: A preliminary study,” *Diagn. Interv. Imaging*, vol. 101, no. 2, pp. 91–100, 2020.
- [34] Z. Zhang, S. Li, Z. Wang, and Y. Lu, “A novel and efficient tumor detection framework for pancreatic cancer via CT images,” in *Proc. 42nd Annu. Int. Conf. IEEE Eng. Med. Biol. Soc. (EMBC)*, 2020, pp. 1160–1164.
- [35] T. A. Qureshi, S. Gaddam, A. M. Wachsman *et al.*, “Predicting pancreatic ductal adenocarcinoma using artificial intelligence analysis of pre-diagnostic computed tomography images,” *Cancer Biomark.*, vol. 33, no. 2, pp. 211–217, 2022.
- [36] W. Mu, C. Liu, F. Gao *et al.*, “Prediction of clinically relevant pancreatico-enteric anastomotic fistulas after pancreatoduodenectomy using deep learning of preoperative computed tomography,” *Theranostics*, vol. 10, no. 21, pp. 9779–9788, 2020.
- [37] L. C. Chu, S. Park, S. Kawamoto *et al.*, “Application of deep learning to pancreatic cancer detection: Lessons learned from our initial experience,” *J. Am. Coll. Radiol.*, vol. 16, no. 9, pp. 1338–1342, 2019.
- [38] Y. Deng, B. Ming, T. Zhou *et al.*, “Radiomics model based on MR images to discriminate pancreatic ductal adenocarcinoma and mass-forming chronic pancreatitis lesions,” *Front. Oncol.*, vol. 11, 620981, 2021.
- [39] K. Si, Y. Xue, X. Yu *et al.*, “Fully end-to-end deep-learning-based diagnosis of pancreatic tumors,” *Theranostics*, vol. 11, no. 8, pp. 1982–1990, 2021.
- [40] M. Ozkan, M. Cakiroglu, O. Kocaman *et al.*, “Age-based computer-aided diagnosis approach for pancreatic cancer on endoscopic ultrasound images,” *Endosc. Ultrasound*, vol. 5, no. 2, p. 101, 2016.
- [41] R. Maskeliūnas, R. Damaševičius, A. Kulikajėvas, E. Padervinskis, K. Pribušis, and V. Uloza, “A hybrid U-Lossian deep learning network for screening and evaluating Parkinson’s disease,” *Appl. Sci.*, vol. 12, no. 22, 11601, 2022.
- [42] C. Quan, K. Ren, Z. Luo, Z. Chen, and Y. Ling, “End-to-end deep learning approach for Parkinson’s disease detection from speech signals,” *Biocybern. Biomed. Eng.*, vol. 42, no. 2, pp. 556–574, 2022.
- [43] A. Yasar, I. Saritas, M. A. Sahman, and A. C. Cinar, “Classification of Parkinson disease data with artificial neural networks,” in *Proc. IOP Conf. Ser. Mater. Sci. Eng.*, vol. 675, 2019, 012031.
- [44] I. Nissar, D. R. Rizvi, S. Masood, and A. N. Mir, “Voice-based detection of Parkinson’s disease through ensemble machine

learning approach: A performance study,” *EAI Endorsed Trans. Pervasive Health Technol.*, vol. 5, no. 19, 162806, 2019.

- [45] L. Yuan, Y. Liu, and H. M. Feng, “Parkinson disease prediction using machine learning-based features from speech signal,” *Serv. Orient. Comput. Appl.*, vol. 18, no. 1, pp. 101–107, 2023.
- [46] R. Mathur, V. Pathak, and D. Bandil, “Parkinson disease prediction using machine learning algorithm,” in *Proc. Emerging Trends in Expert Applications and Security*, 2019, pp. 357–363.

Copyright © 2025 by the authors. This is an open access article distributed under the Creative Commons Attribution License ([CC-BY-4.0](https://creativecommons.org/licenses/by/4.0/)), which permits use, distribution and reproduction in any medium, provided that the article is properly cited, the use is non-commercial and no modifications or adaptations are made.